A Novel Fractional Viscoelastic Constitutive Model for Shape Memory Polymers

Zhouzhou Pan, Zishun Liu

International Center for Applied Mechanics, State Key Laboratory for Strength and Vibration of Mechanical Structures, School of Aerospace, Xi'an Jiaotong University, Xi'an 710049, China
Correspondence to: Z. Liu (E-mail: ZishunLiu@mail.xjtu.edu.cn)

Received 15 April 2018; revised 8 May 2018; accepted 14 May 2018; published online in Wiley Online Library
DOI: 10.1002/polb.24631

ABSTRACT: Shape memory polymers (SMPs) are a class of smart materials which can recover from a deformed shape to their original shape by a certain external stimulus. To predict the deformation behaviors of SMPs, different constitutive models have been developed in the last few years. However, most of the constitutive models need many parameters to be determined by specific experiments and complex calibration processes. This drawback has limited their application in promoting the development of SMPs. Thus, it is imperative to develop a new constitutive model which is not only accurate, but also relatively simple. In our work, a novel fractional viscoelastic constitutive model coupling with time-temperature superposition principle is first proposed for SMPs. Then, frequency sweep and temperature sweep experiments are conducted to determine the parameters of the model. Finally, the shape memory free recovery experiments are carried out to validate the predictive capability of the developed model. By comparing the predicted results with experimental data, we find that though our model has only eleven parameters in total, it could capture the thermomechanical behaviors of SMPs in very good agreement with experimental results. We hope the proposed new model provide researchers with guidelines in designing and optimizing of SMP applications. © 2018 Wiley Periodicals, Inc. J. Polym. Sci., Part B: Polym. Phys. **2018**, *56*, 1125–1134

KEYWORDS: fractional viscoelastic constitutive model; mechanical tests; shape memory polymers; stimuli sensitive polymers; thermomechanical behaviors; time-temperature superposition

INTRODUCTION Shape memory polymers (SMPs) are a class of smart materials that have the ability to fix at a deformed state and then return to their original shape by a certain external stimulus, such as temperature, electricity, light, magnetic field, and so on. Compared to shape memory alloys and shape memory ceramics, SMPs have many unique advantages: low density, easily tailored properties, low cost, and especially large deformation recovery capacity.[1–4] These novel characteristics have put SMPs in the limelight of research arena for the past three decades with investigations focusing toward the potential applications of SMPs, for example, deployable structures, biomedical devices, smart textiles, and self-healing composite systems.[5–9]

Shape memory recovery triggered by temperature is known as thermally induced shape memory effect. The typical thermomechanical circle of thermally induced SMPs can be described as: deform the SMP under external forces at a high temperature; decrease the temperature while maintaining the deformed shape; remove the external forces; reheat the SMP and it recovers to the original shape.[10,11]

Many constitutive models have been developed to describe and predict the thermomechanical behaviors of SMPs. Typically these models could be classified as two categories: phenomenological models and rheological models.[12–15] The phenomenological model based on the phase translation approach was first introduced by Liu et al.,[16] who considered the epoxy-based SMPs was a mixture of frozen phase and active phase, and the volume fractions of the two phases were changed according to the temperature. Under these considerations, they developed a constitutive model which could effectively predict the thermomechanical behavior of the SMP under small strains. The two phase concept was gradually adopted by many researchers to develop new models to improve the predictive capability for the large strain cases. For example, Chen and Lagoudas[9] developed a model for large deformation which combined the phase concept and neo-Hookean rubber elasticity model. Kim et al.[17] added another phase (hard phase) to the two phase model to describe the behavior of shape memory polyurethanes under large strains. The rheological model is based on the inherent viscoelasticity of SMPs and the early models were proposed

© 2018 Wiley Periodicals, Inc.

by Tobushi et al.,[18] Lin and Chen[19] by using linear rheology element (spring elements and dashpot elements). One major shortcoming of these models is that they usually could predict just qualitatively, but not quantitatively. To describe the thermomechanical behavior accurately, researchers improved the simple viscoelastic model by introducing more linear or nonlinear elements.[20] Nguyen et al.[21] presented a new constitutive model by incorporating the nonlinear Adam–Gibbs model of structural relaxation and a modified Eyring model of viscous flow into a continuum finite-deformation thermoviscoelastic framework. Westbrook et al.[22] applied multibranch model (equilibrium branch, glassy nonequilibrium branch, rubbery nonequilibrium branches) including time-temperature superposition to predict SME by considering the complex thermomechanical properties of amorphous SMPs as the temperature crosses the translation temperature T_g. Diani et al.[12] employed the generalized Maxwell model including time-temperature superposition to predict the recovery of the epoxy-based SMP. Li et al.[13] proposed a viscoelastic model based on multiplicative thermoviscoelasticity and defined different constitutive structures for above and below transformation temperature in their model.

Though, both of the above approaches have great significance to promote the application of SMPs, there are limitations that make them complicated to be put into practice. The first type constitutive models fall short of describing the viscoelastic properties of SMPs due to the lack of consideration of the time dependence effect. For the second type, the main limitation is that most of the presented models have many parameters (e.g., more than 23 parameters in the model of Park et al.,[23] 31 in the model of Diani et al.,[12] 42 in the model of Yu et al.,[24] and up to 45 in the model of Srivastava et al.[25] that need to be accurately determined through specific experiments and complex calibration processes. Therefore, it is imperative to develop a new constitutive model by considering both the accuracy and the simplicity.

This work aims to develop a fractional viscoelastic constitutive model with fewer parameters. The classical viscoelastic models, such as Generalized Maxwell and Generalized Kevin-Voigt, are based on constitutive model equations with differential operators of integer order, which provide exponential type relationships between relaxation modulus and time. However, many polymers show a relaxation behavior of power-law type. A large number of elements are required to approximate the relaxation behavior that spans several orders. This leads to a fact that a large number of material parameters should be determined from experiments. In contrast, fractional order formulations have been found to have ability to describe complex viscoelastic behavior with less parameters.[26,27] According to the time-temperature superposition principle, it would require fewer parameters to approximate the relationships between storage modulus and temperature by using a fractional viscoelastic model. Owing to this advantage of the fractional viscoelastic model, significant amount of work has been conducted on the prediction of the deformation property for viscoelastic materials. However, to the authors' best knowledge, little research has been conducted to predict the thermomechanical property of SMP by using fractional differential models. We could only find that Fang et al.[28] tried to apply the fractional calculus methods to viscoelastic response of amorphous SMPs, but they only concentrated on the relaxation properties and the final step instead of the whole complex thermomechanical behavior of SMPs. Hence, we will apply the fractional viscoelastic model to systematically study the thermomechanical behavior of SMPs. At the same time, experiments are also conducted to determine the unknown parameters and verify the accuracy of the presented model.

The paper is organized as follows. The "Experimental" section presents the experimental results of the dynamic frequency sweep tests and the dynamic temperature sweep test. In addition, the coefficient of thermal expansion measurement and shape memory circle of free recovery tests of the SMP are also presented in this section. In the "The novel constitutive model" section, we briefly introduce the theory of fractional calculus and develop a novel fractional viscoelastic model for SMPs. Then the parameters of the model for SMPs are determined in the "Parameters determination" section. The comparisons between the model predictions and experimental results are presented in the "Results and discussion" section. The following section draws the main conclusions of the paper. Finally, the article is completed by an Appendix where the implementation procedure of the constitutive model for each step of the free recovery circle is presented.

EXPERIMENTAL

Materials

The SMP material used in this study is a styrene-based thermosetting polymer, which has potential application in many fields.[29,30] All the materials were purchased from Sigma-Aldrich and used without any purification. In the synthesis process, the styrene (analytical reagent), butyl acrylate (analytical reagent), divinyl-benzene (analytical reagent), and benzoyl peroxide (analytical reagent) were first mixed with mass ratio of 65:35:2:2, then the mixture was stirred with a magnetic stirrer and the mixture was casted into a glass mould. Finally, it was cured in an oven at 70 °C for 24 h. After curing, the SMP sample was machined to rectangular shape with dimension of 20 mm × 5 mm × 0.74 mm.

Dynamic Mechanical Analysis

The dynamic mechanical analysis for SMP was performed on the DMA tester (Q800, TA Instruments, New Castle, DE) using the tensile mode.[31] The glass transition temperature was tested by a dynamic temperature sweep procedure at 1 Hz, and the result is shown in Figure 1. The translation temperature region ranges from 40 °C to 60 °C and the translation temperature corresponding to the peak of the lose angle ($\tan\delta$) curve is about 53.5 °C. The time-temperature dependency of the SMP was determined by using dynamic frequency sweeps for each temperature (stepwise from 30 °C

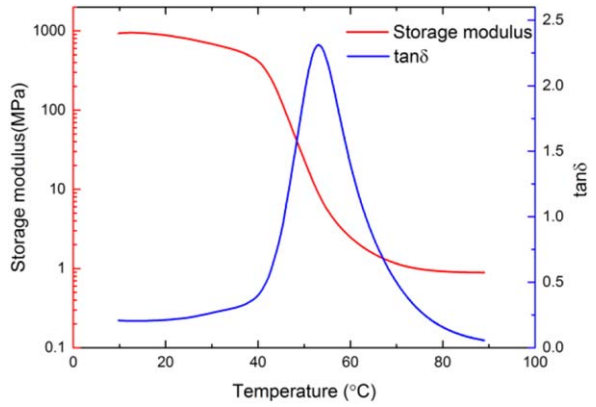

FIGURE 1 The temperature dependent storage modulus and tan δ curves of the polystyrene-based SMP obtained from a temperature sweep test at 1 °C/min and 1 Hz using DMA machine. [Color figure can be viewed at wileyonlinelibrary.com]

to 70 °C with 5 °C increments and the translation temperature) at the frequencies range of 0.01–100 Hz. The storage modulus and tan δ curves as a function of frequency are shown in Figure 2.

CTE Measurement

The coefficient of thermal expansion (CTE) was measured by capturing the strain of SMP specimen under no external force using the DMA tester. To measure the CTE, a SMP sample was first heated to 75 °C at the rate of 1 °C/min and equilibrated at the temperature for 10 min. Then the sample was cooled to 15 °C at the rate of 1 °C/min. At the meanwhile, the strain during the cooling step was recorded. Figure 3 shows the thermal strain evolution during cooling from 75 °C to 15 °C. The CTE α is defined as the slope of the thermal strain curve.

Shape Memory Circle Test

The whole circle of shape memory test was conducted on the DMA tester as well. In the first step, the shape memory rectangular specimen was first deformed to the predefined strain under a strain rate of 2%/min at 65 °C. Subsequently, the deformed specimen was cooled to 20 °C at the temperature dropping rate of 1 °C/min while maintaining the total strain unchanged. Then the external force was removed and the temporary (deformed) shape was retained. Finally, the SMP was reheated to 65 °C at the rate of 2 °C/min. Meanwhile, the temporary shape was recovered to the original shape. The stress train temperature curves of the SMP at 5% strain and 10% strain are shown in Figure 4.

THE NOVEL CONSTITUTIVE MODEL

Preliminaries: Fractional Calculus

The theory of fractional calculus deals with integrals and derivatives of non-integer order. There are different definitions of fractional operators and the detailed information

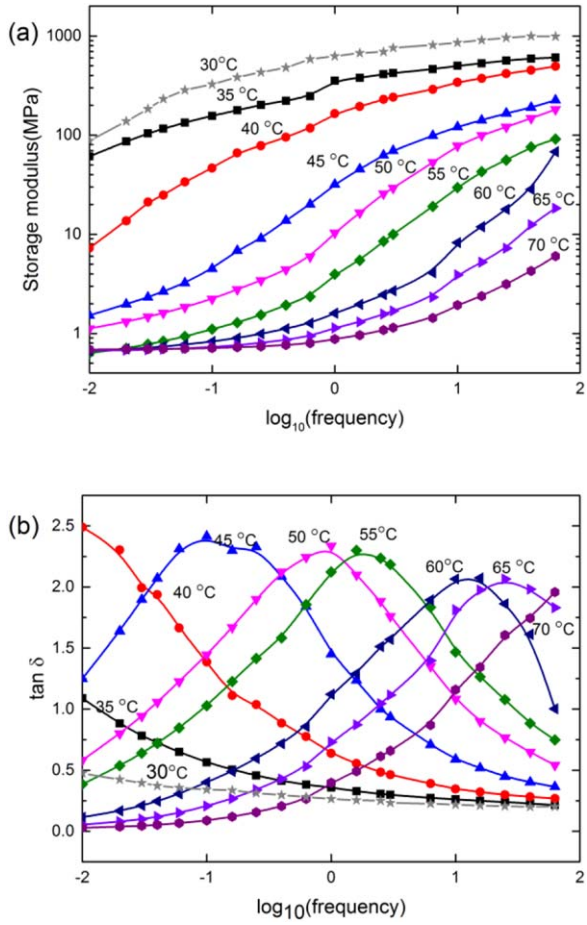

FIGURE 2 (a) Storage modulus and (b) tan δ as a function of frequency at varying temperatures from 0.01 Hz to 100 Hz obtained from frequency sweep tests using DMA machine. [Color figure can be viewed at wileyonlinelibrary.com]

could be found in the work of Mainardi.[32] Among these definitions, Riemann–Liouville fractional integral operator is the most commonly used and its definition which is based on

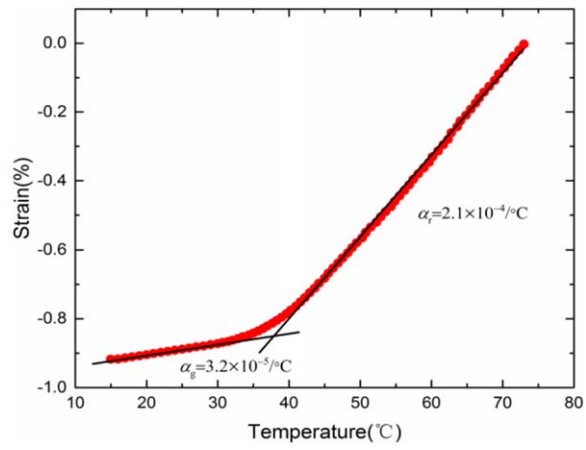

FIGURE 3 Thermal expansion strain as a function of temperature. [Color figure can be viewed at wileyonlinelibrary.com]

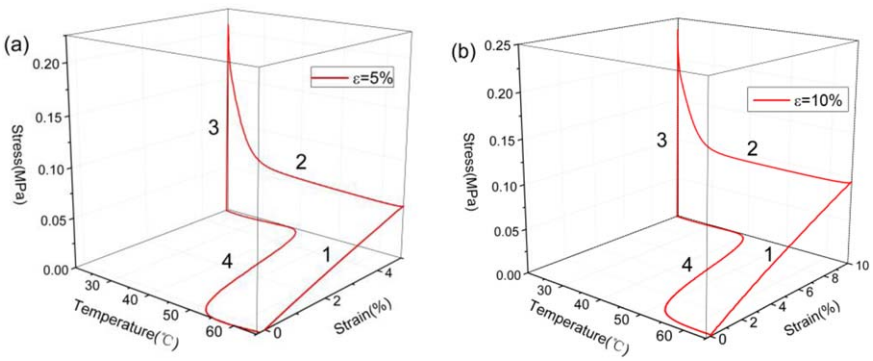

FIGURE 4 Thermomechanical free recovery test at pre-strain of (a) 5% and (b) 10%. (1) Uniaxial tension at 65 °C; (2) cooling the specimens to 20 °C at the dropping rate of 1 °C/min while keeping the strain unchanged; (3) remove the external force; (4) reheating the specimen at the heating rate of 2 °C/min. [Color figure can be viewed at wileyonlinelibrary.com]

the Cauchy formula for repeated integration shows as follows:

$$J^{\beta}f(t)=\frac{1}{\Gamma(\beta)}\int_0^t(t-\tau)^{\beta-1}f(\tau)d\tau, t>0, \beta\in\mathbb{R}^+ \tag{1}$$

where J^{β} is a fractional integral operator, β is order of the fractional integral, $\mathbb{R}^+$ is the set of positive real numbers, $f(\tau)$ is an integrand, and $\Gamma(\beta)$ is the Gamma function which is defined by:

$$\Gamma(\beta)=\int_0^{\infty}\mathrm{e}^{-t}t^{\beta-1}dt \tag{2}$$

The derivatives are the inverse operator to integrals and there are two definitions of the fractional derivative. The first is defined by Riemann–Liouville as left-inverse to the fractional integral; the second is defined by Caputo as left-inverse to the fractional integral. In general, the latter is more popular in dealing with viscoelasticity because the Caputo derivative of a constant is zero and the Caputo fractional derivative appears more suitable to be treated by the Laplace transform technique in that it requires the knowledge of the bounded initial values of the function. Therefore, we use Caputo derivative in this work and it is defined by:

$$D^{\beta}f(t)=\begin{cases}\dfrac{1}{\Gamma(m-\beta)}\displaystyle\int_0^t(t-\tau)^{m-1-\beta}f^{(m)}(\tau)d\tau, m-1<\beta<m\\ \dfrac{d^m}{dt^m}f(t), \beta=m\end{cases} \tag{3}$$

where D^{β} is a fractional derivative operator, m is a positive integer.

Transforming the abolve derivation into Lapalace complex domain, we obtain:

$$L\{D^{\beta}f(t)\}=s^{\beta}\tilde{f}(s)-\sum_{i=0}^{m-1}s^{\beta-1-i}f^{(i)}(0^+)s\in\mathbb{C} \tag{4}$$

where $\mathbb{C}$ is the set of complex numbers.

Fractional Viscoelastic Model

The schematic of the proposed new constitutive model is shown in Figure 5. In the model, we consider that the effect of thermal expansion on the thermomechanical behavior of SMPs is independent on the mechanical behaviors. Therefore, the total strain of the SMP can be written as the summation of the mechanical strain ε_M and the thermal strain ε_T, that is,

$$\varepsilon_{\mathrm{Total}}=\varepsilon_M+\varepsilon_T \tag{5}$$

For the thermal part, it is defined by:

$$\varepsilon_T=\alpha(T-T_0) \tag{6}$$

where α is the coefficient of thermal expansion (CTE), T_0 is the reference temperature. T is the present temperature. To capture the deformation behavior of SMPs, two fractional Maxwell elements (nonequilibrium branches) and a Hookean spring (equilibrium branch) are arranged in parallel. Like generalized Maxwell model (GMM), the present model could be named as the generalized fractional Maxwell model (GFMM). In the equilibrium branch, the stress σ_{eq} and strain $\varepsilon_{\mathrm{eq}}$ follows the linear elastic principle:

$$\sigma_{\mathrm{eq}}=E_{\mathrm{eq}}\varepsilon_{\mathrm{eq}}(t) \tag{7}$$

where E_{eq} is the stiffness of the spring in equilibrium branch. In each fractional Maxwell element (nonequilibrium branch), it consists of a linear spring and a spring-spot. In the spring-spot, the stress σ_{ss} and strain $\varepsilon_{\mathrm{ss}}$ obeys the following rule:

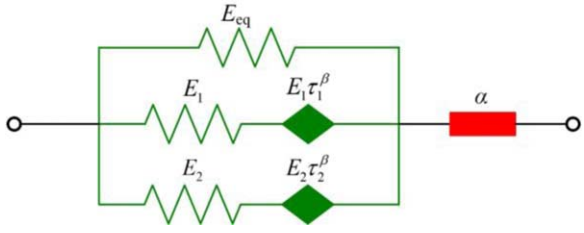

FIGURE 5 Schematic of generalized fractional viscoelastic model for SMPs. [Color figure can be viewed at wileyonlinelibrary.com]

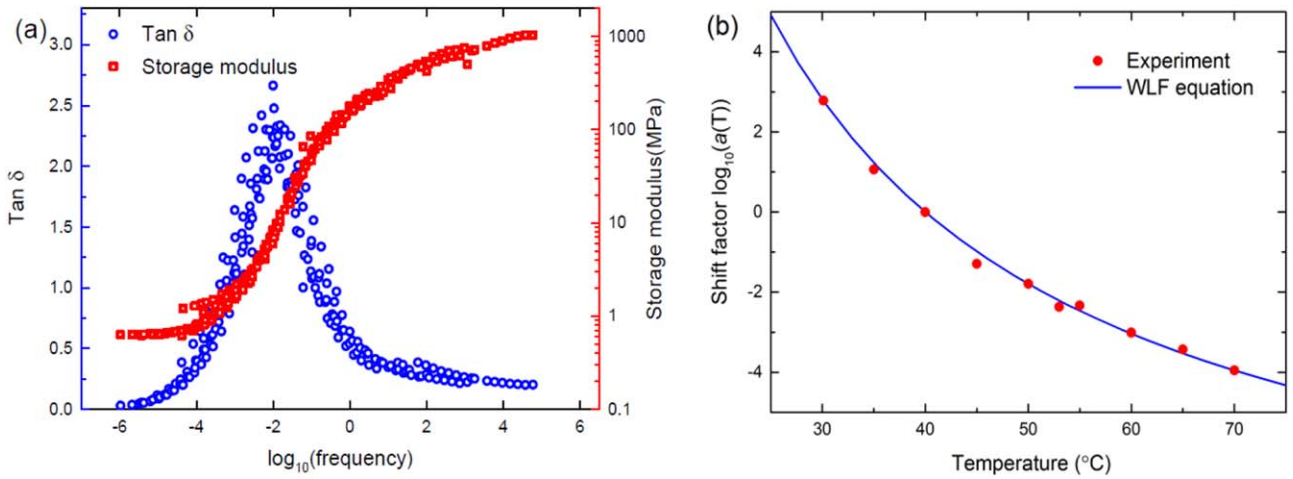

FIGURE 6 (a) Storage modulus and tan δ master curves of the SMP obtained from horizontally shifting the frequency sweep tests in Figure 2 using a reference temperature of 40 °C; (b) WLF equation approximation of the shift factors. [Color figure can be viewed at wileyonlinelibrary.com]

$$\sigma_{ss}=E\tau^{\beta}\frac{D^{\beta}\varepsilon_{ss}(t)}{Dt^{\beta}},0<\beta<1 \tag{8}$$

where E is the stiffness of the spring, τ is the relaxation time, and β is a decimal between 0 and 1. Then, the fractional differential equation of each fractional Maxwell element can be expressed as:

$$\frac{D^{\beta}\sigma_{FM}}{Dt^{\beta}}+\frac{1}{\tau^{\beta}}\sigma_{FM}=E\frac{D^{\beta}\varepsilon_{FM}}{Dt^{\beta}},0<\beta<1 \tag{9}$$

where σ_{FM} and ε_{FM} are stress and strain in a fractional Maxwell element, respectively. The explicit stress–strain relationship of the fractional Maxwell element can be solved by Laplace transform and is given by,

$$\begin{aligned}\sigma_{FM}(t)=&E\int_{t_0}^{t}E_{\beta}\left(-\left(\frac{(t-\xi)}{\tau}\right)^{\beta}\right)\frac{d\varepsilon_{FM}(\xi)}{d\xi}d\xi\\&+E_{\beta}\left(-\left(\frac{t-t_0}{\tau}\right)^{\beta}\right)\sigma_{FM}(t_0)\end{aligned} \tag{10}$$

where t_0 is the initial time, $\sigma_{FM}(t_0)$ is the initial stress in the fractional Maxwell element and E_{β} is the Mittag-Leffler function:

$$E_{\beta}(x)=\sum_{n=0}^{\infty}\frac{x^n}{\Gamma(\beta n+1)} \tag{11}$$

where n belongs to the set of integers. Finally, the governing equation of the proposed model is:

$$\begin{aligned}\sigma_M(t)=&\sigma_{eq}(t)+\sum_{i=1}^{m}\sigma_i(t)\\=&E_{eq}\varepsilon_M(t)+\sum_{i=1}^{2}\left[E_i\int_{t_0}^{t}E_{\beta}\left(-\left(\frac{(t-\xi)}{\tau_i}\right)^{\beta}\right)\frac{d\varepsilon_M(\xi)}{d\xi}d\xi+\right.\\&\left.E_{\beta}\left(-\left(\frac{t-t_0}{\tau_i}\right)^{\beta}\right)\sigma_i(t_0)\right]\end{aligned} \tag{12}$$

where σ_M is the total mechanical stress.

As the temperature is varied in the thermomechanical circle of SMPs, the variation of the time with changing temperatures should be taken into consideration. Thus, time-temperature superposition principle needs to be coupled with the fractional viscoelastic constitutive model. For thermorheologically simple materials, the shift factor for each branch follows the same rule, and in each branch the effect of changing temperature is simply to horizontally shift the viscoelastic response as a function of frequency,[33] that is,

$$a(T)=\frac{\tau(T)}{\tau(T_r)} \tag{13}$$

where τ (T_r) is the reference relaxation time at the reference temperature T_r, and $a(T)$ is the time-temperature shift factor. The shift factor is commonly used by empirical equations, among which the Williams–Landel–Ferry (WLF) equation shown in eq 14 is the most commonly used.

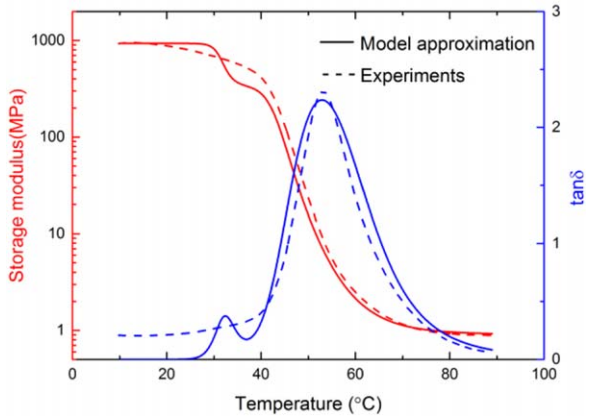

FIGURE 7 Comparisons of the storage modulus and tan δ between model approximations and experiments. [Color figure can be viewed at wileyonlinelibrary.com]

TABLE 1 Material Parameters

Material Parameters	Values	Unit
E_{eq}	0.90	MPa
E_1	336.77	MPa
E_2	596.56	MPa
τ_1	0.6065	s
τ_2	0.0008	s
β	0.793	–
c_1	9.91	–
c_2	45.23	°C
T_r	40	°C
α_r	2.1e-4	$°C^{-1}$
α_g	3.2e-5	$°C^{-1}$

$$\log(a(T)) = \frac{-c_1(T-T_r)}{c_2+(T-T_r)} \tag{14}$$

where c_1 and c_2 are material constants that depend on the reference temperature T_r.

PARAMETERS DETERMINATION

In this study, the reference temperature T_r is selected as 40 °C; shift factors are obtained by shifting the storage modulus-frequency curves measured at different temperatures into a master curve. The master curves are shown in Figure 6(a). Then, the parameters c_1 and c_2 in the WLF equation are determined by fitting the equation with the shift factors. The shift factors and WLF equation fitting results are shown in Figure 6(b).

To determine the material parameters E_{eq}, E_i, τ_i, β, the storage modulus and tan δ derived from our fractional viscoelastic model are employed to fit with the dynamic temperature sweep test curve at 1 Hz. The complex modulus E^* of a fractional Maxwell model as a function of angular frequency ω is:

$$\begin{aligned} E^*(\omega) &= \left(\frac{1}{E}+\frac{1}{E(i\omega\tau)^\beta}\right)^{-1} = E\frac{(i\omega\tau)^\beta}{1+(i\omega\tau)^\beta} \\ &= E\frac{(\omega\tau)^{2\beta}+(\omega\tau)^\beta\cos(\beta\pi/2)}{1+(\omega\tau)^{2\beta}+2(\omega\tau)^\beta\cos(\beta\pi/2)} \\ &+ iE\frac{(\omega\tau)^\beta\sin(\beta\pi/2)}{1+(\omega\tau)^{2\beta}+2(\omega\tau)^\beta\cos(\beta\pi/2)} \end{aligned} \tag{15}$$

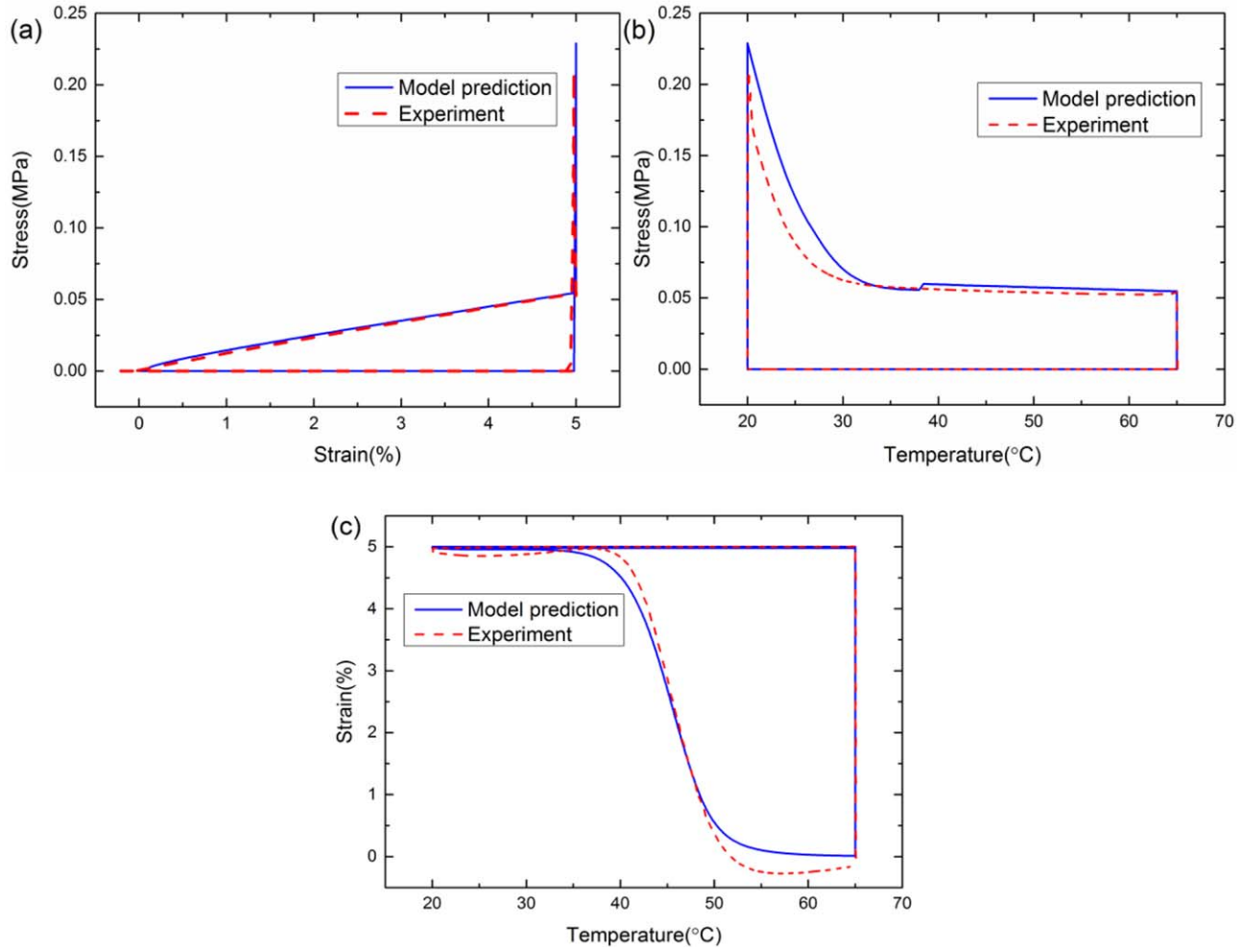

FIGURE 8 The comparisons between model predictions and experiments for the whole circle of free recovery at pre-strain of 5%: (a) stress–strain curves; (b) stress–temperature curves; (c) strain–temperature curves. [Color figure can be viewed at wileyonlinelibrary.com]

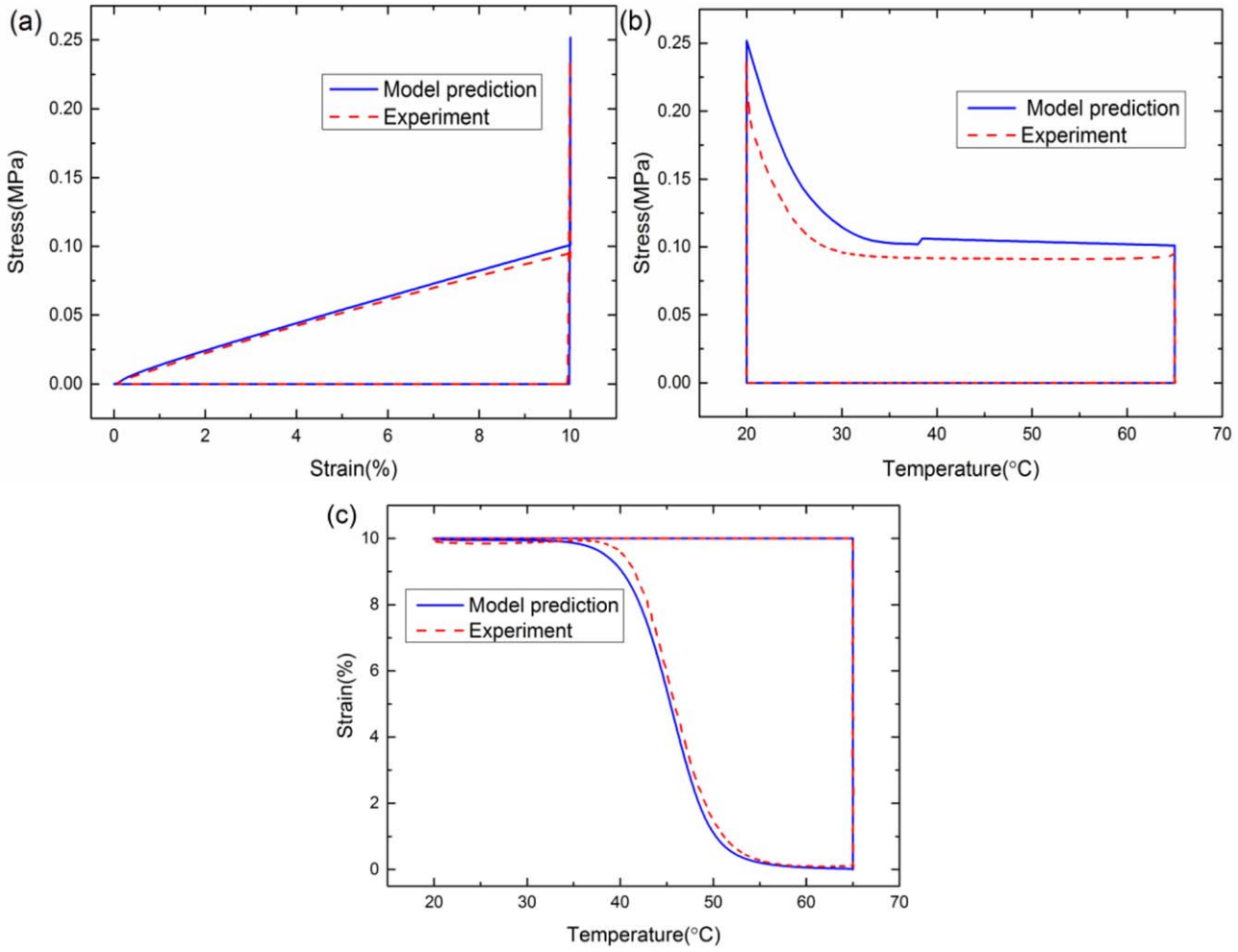

FIGURE 9 The comparisons between model predictions and experiments for the whole circle of free recovery at pre-strain of 10%: (a) stress–strain curves; (b) stress–temperature curves; (c) strain–temperature curves. [Color figure can be viewed at wileyonlinelibrary.com]

Thus, the temperature dependent storage modulus E', lose modulus E'' and the lose angle tan δ of the GFMM are:

$$E'(\omega,T)=E_{\mathrm{eq}}+\sum_{i=1}^{m}E_i\frac{(\omega\tau_i)^{2\beta}+(\omega\tau_i)^{\beta}\cos(\beta\pi/2)}{1+(\omega\tau_i)^{2\beta}+2(\omega\tau_i)^{\beta}\cos(\beta\pi/2)} \tag{16}$$

where ω is equal to 2π and $\tau_i=a(T)\tau_i(T_r)$. Then the parameters E_{eq}, E_i, τ_i, β are obtained by fitting with the curves of storage modulus and lose factor as a function of temperature. The storage modulus and lose factor curves predicted by the present model and experiments are shown in Figure 7. The coefficient of thermal expansion for polystyrene is obtained by calculating the slope of the thermal strain curve at glassy state and rubber state, respectively. Up to now, all the parameters of the model are obtained and listed in Table 1. The parameters will be used later directly for predicting the thermomechanical properties of the SMPs.

RESULTS AND DISCUSSION

To show the ability of the proposed model in predicting the thermomechanical property of SMPs, the experiments of shape memory circle for polystyrene-based SMPs with different pre-strains are conducted to provide for comparison. During the numerical prediction process, the equations in the implementation procedures of the constitutive model part (shown in Appendix) are implemented into the MATLAB program and all the conditions are set the same with the experiments in the section of "Experimental." The parameters used in the constitutive model are shown in Table 1 and no additional fitting is required in predicting the shape memory free recovery circle. The comparisons of stress–strain curves, stress–temperature curves, and strain–temperature curves between model predictions and experiments are shown in Figures 8 and 9 for 5% pre-strain and 10% pre-strain, respectively. It shows that the fractional viscoelastic model could predict in good agreement with the experimental observations for different levels of pre-deformation.

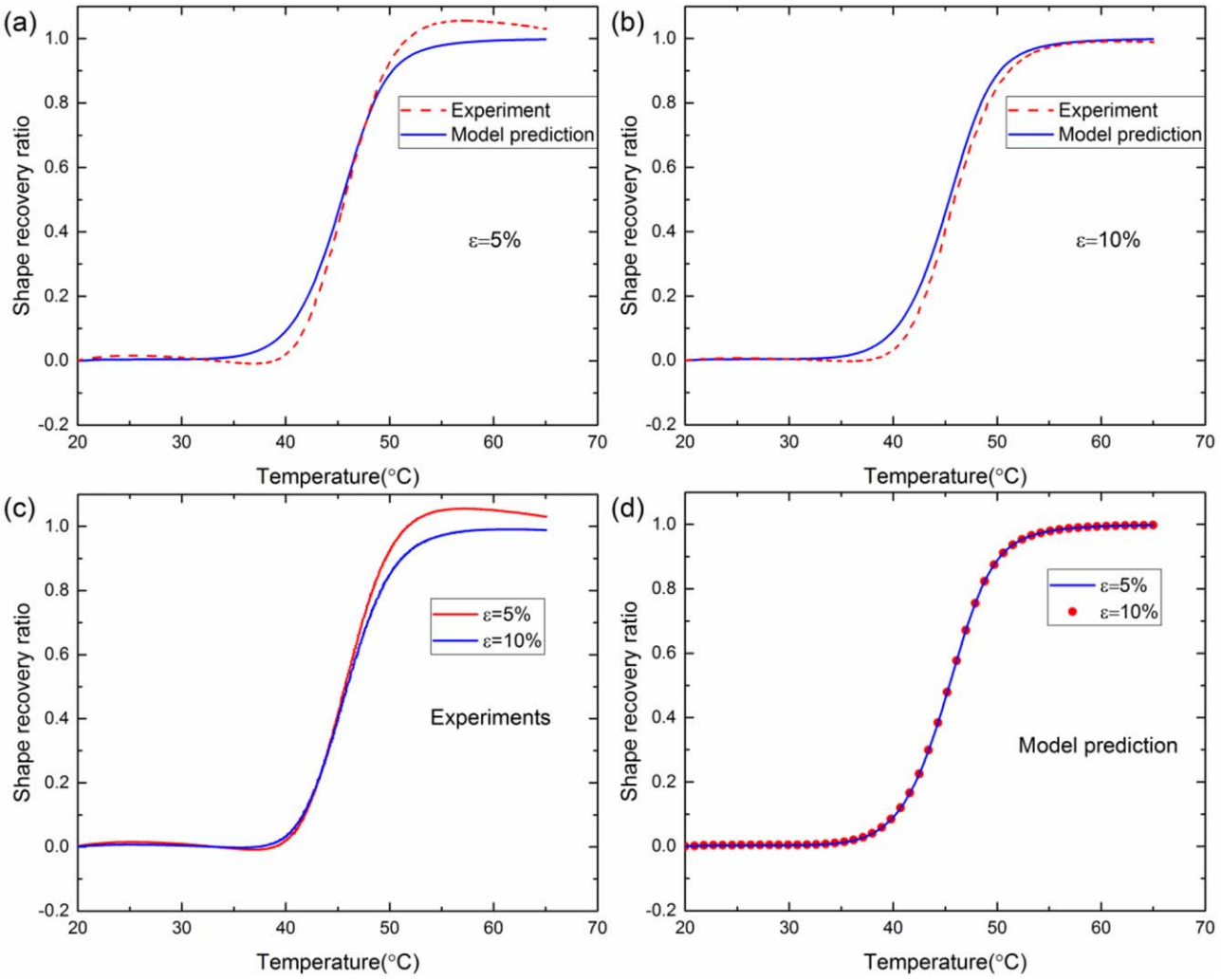

FIGURE 10 The shape recovery ratio with respect to temperature for comparison between: (a) experiments and predictions under prestrain of 5%; (b) experiments and predictions under prestrain of 10%; (c) experiments under prestrain of 5% and 10%; (d) predictions under prestrain of 5% and 10%. [Color figure can be viewed at wileyonlinelibrary.com]

To quantitatively describe the shape recovery property, the shape recovery ratio is defined by the recovered strain over the fixed strain:[34]

$$R_r = 1 - \frac{\varepsilon(T)}{\varepsilon(T_3)} \tag{17}$$

where $\varepsilon(T_3)$ is the value of strain measured at the start of the free recovery process. Figure 10(a,b) shows the comparison of experimental results with predictions for shape recovery ratio under pre-strain of 5% and 10%. By further plotting the shape recovery ratio with respect to temperature for 5% pre-strain and 10% pre-strain in the same graph, we find that both the experiments shown in Figure 10(c) and the model prediction shown in Figure 10(d) demonstrate that the shape recovery ratio shows almost the same evolution in spite of the value of the pre-strain for the polystyrene-based SMP. The same results are also found by Arrieta et al.[35] for an acrylate-based SMP. This finding may provide guidelines for developing SMP applications.

CONCLUSIONS

Constitutive models for SMPs are fundamental for the development of SMP applications. In this paper, a novel fractional viscoelastic model coupling with the time-temperature superposition principle is developed for simulating the thermomechanical behaviors of SMPs. The frequency sweep experiments are conducted to determine the parameters c_1 and c_2 in the WLF equation and the temperature sweep tests are carried out to identify the material parameters E_{eq}, E_i, τ_i, β_i. Then the shape memory free recovery experiments for a polystyrene-based SMP are carried out to validate the predictive capability of the model. Though our model has only three branches (one equilibrium branch and two nonequilibrium branches) and eleven parameters in total, it could

capture the thermomechanical behaviors of SMPs in very good agreement with experimental results of shape memory free recovery. It should be noted that both the theoretical predictions and experimental results demonstrate that the shape recovery ratio shows almost the same evolution in spite of the value of the pre-strain.

APPENDIX: IMPLEMENTATION PROCEDURES OF THE CONSTITUTIVE MODEL

In this part, we present the implementation method to solve eq 12 for each step of the shape memory circle. Due to the fact that the whole circle of the shape memory behavior consists of four different steps, we have to implement the equation step by step. In the first step, it is a strain controlled loading process with constant strain rate $\dot{\varepsilon}_1$ and the initial strain is zero. Thus, eq 12 could be simplified as:

$$\sigma_M(t)=E_{eq}\dot{\varepsilon}_1 t+\dot{\varepsilon}_1\sum_{i=1}^{2}E_i\left[\int_0^t E_\beta\left(-\left(\frac{(t-\xi)}{\tau_i}\right)^\beta\right)d\xi\right]. \quad \text{(A1)}$$

Then the temperature is decreasing at the rate of $\dot{T}_2$ while the total strain is maintained. According to eqs 5 and 6, the mechanical strain is increased at a rate of $\dot{\varepsilon}_2=\alpha\dot{T}_2$. At thiscondition, the governing equation could be rewritten as:

$$\sigma_M(t)=E_{\mathrm{eq}}\dot{\varepsilon}_2\cdot(t-t_1)+\sum_{i=1}^{2}\left[E_i\dot{\varepsilon}_2\int_{t_1}^{t}E_\beta\left(-\left(\frac{(t-\xi)}{\tau_i(T)}\right)^\beta\right)d\xi+E_\beta\left(-\left(\frac{t-t_1}{\tau_i(T)}\right)^\beta\right)\sigma_i(t_1)\right] \quad \text{(A2)}$$

where t_1 is the initial time of the second step. Subsequently, in the third step, the external force is removed instantly and there is a small springback of strain $\Delta\varepsilon\varepsilon$. To calculate the $\Delta\varepsilon$, we write the total stress in another form:

$$\sigma=E_{\mathrm{eq}}\varepsilon_{\mathrm{eq}}+\sum_{i=1}^{2}E_i\varepsilon_i^{\mathrm{e}} \quad \text{(A3)}$$

where $\varepsilon_i^{\mathrm{e}}$ denotes the strain of the spring in the nonlinear branches.

Since the total stress is decreased to zero instantly, we assume the $\Delta\varepsilon$ results from the spring. Then the following equation holds:

$$0=E_{\mathrm{eq}}\left(\varepsilon_{\mathrm{eq}}-\Delta\varepsilon\right)+\sum_{i=1}^{2}E_i\left(\varepsilon_i^{\mathrm{e}}-\Delta\varepsilon\right) \quad \text{(A4)}$$

The above equation can also be written as:

$$\Delta\varepsilon=\frac{E_{\mathrm{eq}}\varepsilon_{\mathrm{eq}}+\sum_{i=1}^{2}E_i\varepsilon_i^{\mathrm{e}}}{E_{\mathrm{eq}}+\sum_{i=1}^{2}E_i} \quad \text{(A5)}$$

Realizing that the numerator in eq A5 is the total stress σ_2 just before unloading, thus eq A5 can be further written as:

$$\Delta\varepsilon=\frac{\sigma_2}{E_{\mathrm{eq}}+\sum_{i=1}^{2}E_i} \quad \text{(A6)}$$

Finally, the SMP is reheated to the high temperature without any constraints and it can recover most of the deformed strain to its original state. During the process, the total stress maintains at zero:

$$0=E_{\mathrm{eq}}\varepsilon_{\mathrm{eq}}+\sum_{i=1}^{2}E_i\varepsilon_i^{\mathrm{e}} \quad \text{(A7)}$$

In each Fractional Maxwell element, the stress is identical in the spring and spring-spot elements:

$$E_i\varepsilon_i^{\mathrm{e}}=E_i\tau_i^\beta\frac{D^\beta\varepsilon_i(t)}{Dt^\beta} \quad \text{(A8)}$$

Owing to the parallel arrangement of the equilibrium branch and nonequilibrium branch, the strain in nonequilibrium branch is equal to that in the equilibrium branch:

$$\varepsilon_{\mathrm{eq}}=\varepsilon_i^{\mathrm{e}}+\varepsilon_i^{v} \quad \text{(A9)}$$

where ε_i^{v} denotes the strain in the spring-spot element.

Substituting eqs A8 and A[9] into eq A7, we obtain the system equations:

$$[E]\left\{\frac{D^\beta\varepsilon^{\mathrm{e}}}{Dt^\beta}\right\}=-\frac{1}{a(T(t))}[B]\{\varepsilon^{\mathrm{e}}\} \quad \text{(A10)}$$

where $E_{\mathrm{ij}}=E_{\mathrm{j}}/E_{\mathrm{eq}}+\delta_{\mathrm{ij}}$, $B_{\mathrm{ij}}=\delta_{\mathrm{ij}}/\tau_{\mathrm{i}}$, and δ_{ij} is the Kronecker Delta. Realizing that the above equations are coupled and could not be solved individually, we calculate them by using the diagonalization method. The details can be found in any linear algebra book.

The above equations are implemented into the MATLAB program for predicting the thermomechanical behaviors of SMPs.

ACKNOWLEDGMENT

Authors are grateful for the support from the National Natural Science Foundation of China (11572236).

REFERENCES AND NOTES

1 Y. He, S. Guo, Z. Liu, K. M. Liew, *Int. J. Solids Struct.* **2015**, *71*, 194.

2 G. Li, W. Xu, *J. Mech. Phys. Solids* **2011**, *59*, 1231.

3 S. Zheng, Z. Li, Z. Liu, *Int. J. Mech. Sci.* **2018**, *137*, 263.

4 R. W. Mailen, M. D. Dickey, J. Genzer, M. A. Zikry, *J. Polym. Sci. Part B: Polym. Phys.* **2017**, *55*, 1207.

5 Y. He, Y. Zhou, Z. Liu, K. M. Liew, *Mater. Des.* **2017**, *132*, 375.

6 F. Li, L. Liu, X. Lan, T. Wang, X. Li, F. Chen, W. Bian, Y. Liu, J. Leng, *Int. J. Appl. Mech.* **2016**, *8*, 1640009.

7 Z. Liu, W. Toh, T. Y. Ng, *Int. J. Appl. Mech.* **2015**, *07*, 1530001.

8 S. M. Hasan, L. D. Nash, D. J. Maitland, *J. Polym. Sci. Part B: Polym. Phys.* **2016**, *54*, 1300.

9 Y.-C. Chen, D. C. Lagoudas, *J. Mech. Phys. Solids* **2008**, *56*, 1752.

10 Z. Pan, R. Huang, Z. Liu, *Polym. Compos.* Doi:10.1002/pc.24658.

11 Q. Zhao, H. J. Qi, T. Xie, *Prog. Polym. Sci.* **2015**, *49–50*, 79.

12 J. Diani, P. Gilormini, C. Frédy, I. Rousseau, *Int. J. Solids Struct.* **2012**, *49*, 793.

13 Y. Li, Y. He, Z. Liu, *Int. J. Plast.* **2017**, *91*, 300.

14 M. Molaaghaie-Roozbahani, N. Heydarzadeh, M. Baghani, A. H. Eskandari, M. Baniassadi, *Int. J. Appl. Mech.* **2016**, *08*, 1650063.

15 Y. Li, J. Hu, Z. Liu, *Int. J. Solids Struct.* **2017**, *124*, 252.

16 Y. Liu, K. Gall, M. L. Dunn, A. R. Greenberg, J. Diani, *Int. J. Plast.* **2006**, *22*, 279.

17 J. H. Kim, T. J. Kang, W.-R. Yu, *Int. J. Plast.* **2010**, *26*, 204.

18 H. Tobushi, T. Hashimoto, S. Hayashi, E. Yamada, *J. Intel. Mater. Syst. Struct.* **1997**, *8*, 711.

19 J. R. Lin, L. W. Chen, *J. Polym. Res.* **1999**, *6*, 35.

20 R. Xiao, C. M. Yakacki, J. Guo, C. P. Frick, T. D. Nguyen, *J. Polym. Sci. Part B: Polym. Phys.* **2016**, *54*, 1405.

21 T. D. Nguyen, C. M. Yakacki, P. D. Brahmbhatt, M. L. Chambers, *Adv. Mater.* **2010**, *22*, 3411.

22 K. K. Westbrook, P. H. Kao, F. Castro, Y. Ding, H. Jerry Qi, *Mech. Mater.* **2011**, *43*, 853.

23 H. Park, P. Harrison, Z. Guo, M.-G. Lee, W.-R. Yu, *Mech. Mater.* **2016**, *93*, 43.

24 K. Yu, H. Li, A. J. W. McClung, G. P. Tandon, J. W. Baur, H. J. Qi, *Soft Matter* **2016**, *12*, 3234.

25 V. Srivastava, S. A. Chester, L. Anand, *J. Mech. Phys. Solids* **2010**, *58*, 1100.

26 S. Müller, M. Kästner, J. Brummund, V. Ulbricht, *Comput. Mater. Sci.* **2011**, *50*, 2938.

27 M. Paggi, A. Sapora, *Int. J. Photoenergy* **2015**, *2015*, 1.

28 C. Q. Fang, H. Y. Sun, J. P. Gu, *J. Mech.* **2015**, *31*, 427.

29 J. Leng, D. Zhang, Y. Liu, K. Yu, X. Lan, *Appl. Phys. Lett.* **2010**, *96*, 111905.

30 R. Liu, Y. Li, Z. Liu, *Mech Time-Depend Mater.* **2018**. Doi: 10.1007/s1104.

31 S. Zheng, Z. Liu, *J. Appl. Mech.* **2017**, *85*, 021002.

32 F. Mainardi, Fractional calculus and waves in linear viscoelasticity: An introduction to mathematical models; Imperial College Press, London, **2010**; pp 1–12.

33 S. W. Katicha, G. W. Flintsch, *Rheol. Acta* **2012**, *51*, 675.

34 Y. C. Sun, S. Y. Cai, J. Ren, H. E. Naguib, *J. Polym. Sci. Part B: Polym. Phys.* **2017**, *55*, 1197.

35 J. S. Arrieta, J. Diani, P. Gilormini, *Smart Mater. Struct.* **2014**, *23*, 095009.